



# One pot easy synthesis and optical characterization of Cd<sub>1-x</sub>Co<sub>x</sub>S/rGO composites starting from graphite oxide by co precipitation method and its electrochemical Properties

Subramani Dorothy<sup>1,2</sup>, Kaliaperumal Punithamurthy<sup>3</sup>, Kaveri Satheesh<sup>4\*</sup>

<sup>1</sup>Department of Chemistry, Bharath University, Chennai, India - 600 073

<sup>2</sup>Bharathiyar University, Coimbatore, India - 641 046

<sup>3</sup>Department of Chemistry, Dhanalakshmi College of Engineering, Tambaram, Chennai, India - 601 301

<sup>4</sup>Research and Development, Department of Physics, Dhanalakshmi College of Engineering, Tambaram, Chennai, India - 601 301

**Abstract:** Cd<sub>(1-x)</sub>Co<sub>(x)</sub>S/rGO nanocomposites were synthesized by an easy and simple one-pot co-precipitation method. The composites were characterized by using X-ray diffractometer (XRD), Fourier transform infrared (FTIR), Raman spectroscopy, Thermogravimetric Analysis (TGA). The presence of elements was confirmed by X-ray photoelectron spectroscopy. The morphological studies FE-SEM and TEM shows that the Cd<sub>(1-x)</sub>Co<sub>(x)</sub>S nanoparticles were deposited on the surface of reduced graphene oxide sheets. The electrochemical property was studied by CV analysis, which indicates the introduction of Co ions into CdS nanoparticles on to the rGO sheets results the increase in the integral area and current. This material could be useful for energy storage devices.

**Keywords:** Cd<sub>(1-x)</sub>Co<sub>(x)</sub>S/rGO, composites, Co-precipitation, Optical properties, Electrochemical property.

## Introduction

In view of increasing serious demand energy and environmental problems, many researchers and scientists have studied electrochemical properties and photocatalytic activity of the materials. Among all the carbon materials, reduced form of graphene oxide (rGO) is used as a supporting material to enhance their properties because of its high surface area, electron transfer kinetics, high stability and good mechanical strength<sup>1</sup>. Reduced graphene oxide is prepared from natural graphite powder by oxidizing (acid treatment) to create functional groups on the surface of the graphene oxide layers. This oxygen containing functional groups offers to deposit other semiconductor material on the surface of layers. The promising properties of reduced graphene oxide and nanoparticles make graphene based hybrid materials are an ideal candidate for the incorporation of variety of functional materials and its application in the area of electrochemistry, photocatalysis, energy and sensors<sup>2-5</sup>.

Doping transition metal ions into the semiconductor nanoparticles have been widely investigated in recent years because of its unusual changes in their properties. By tuning the optical, electrical and magnetic properties of some nanostructures by varying their sizes, structures and morphology has been extensively studied<sup>6-8</sup>. Among the semiconductor materials, Cadmium sulfide is one of the most important chalcogenide

materials which are having a direct band gap of 2.42 eV at room temperature. Now days this material has been widely used for optoelectronic devices. Binary semiconductor nanostructures have been successfully immobilized on reduced graphene oxide sheets or graphene sheets by different methods and reported. But still there is one difficult to control the particle size in the binary semiconductor nanocomposites, which leads to size dependent optical properties and composition dependent optical properties.

In this work, Co (Cobalt) is used as a dopant in to CdS nanoparticles and deposited on reduced graphene oxide sheets. Thiourea is used as a sulfur source as well as reducing agent<sup>9</sup>. Cd<sub>(1-x)</sub>Co<sub>x</sub>S/rGO composites were synthesized by easy and simple co precipitation method and the Characterization was extensively studied. This combined approach opens up the new path for the new technological applications.

## Experimental

### Synthesis of Graphite Oxide and Cd<sub>(1-x)</sub>Co<sub>x</sub>S/rGO composite

Graphite Oxide (GO) was synthesized from graphite powder by using Hummer's method. Cadmium acetate, cobalt acetate and thiourea were used to synthesis Cd<sub>(1-x)</sub>Co<sub>x</sub>S/rGO composites. All the chemicals were used as received without any further purification. 100 mg of GO was dispersed in dehydrated ethanol by ultrasonication for one hour; homogeneous graphene oxide dispersion was obtained and used for the further reactions. 0.05 mol. of cadmium acetate, 0.05 mol. of thiourea and (5% to 20 wt %) cobalt acetate was added to the solution under stirring. The reaction was performed at 60°C for 4 h. After 4 h, the precipitate was filtered and washed by ethanol and water three times. The washed products were centrifuged at 7000 rpm for 10 mins. Then the powder was dried in a vacuum oven for 12 h at 60°C. The final product was calcined at 250°C for 5 h.

### Characterization

The structure of the composite materials was recorded by powder X-ray diffraction (XRD) using Rigaku Rintz Ultima+ with CuK $\alpha$  radiation ( $\lambda=1.54056\text{nm}$ ) at the scanning rate of  $0.5^\circ \text{min}^{-1}$  with X-ray tubes voltage and electric current were 40kV and 20 mA respectively. Fourier transform infrared (FTIR) study for the prepared materials were performed by Perkin Elmer (spectrum 100 FTIR spectrometer) using KBr pellets in the frequency range  $4000 \text{cm}^{-1}$  to  $400 \text{cm}^{-1}$ . Raman Spectra were carried out using Horiba-Jobin Yuon instrument with a 514 nm (Green laser) from  $100 \text{cm}^{-1}$  to  $2000 \text{cm}^{-1}$ . The morphology of the composites was examined through Transmission electron microscopy (TEM- JEOL JEM 2100). Thermal properties of samples were analyzed by Thermogravimetry (TG) measurements using SII EXSTAR 6000 with TG/DTA6200 thermogravimetric analyzer from 40 to  $1000^\circ \text{C}$  at the heating rate of  $5^\circ \text{C}/\text{min}$  using sealed platinum pans under N<sub>2</sub> flow. The presence of the elements and their binding energies in the composites were analyzed by X-ray photoelectron spectroscopy recorded on Theta Probe- Thermo Fisher scientific Inc. X-ray photoelectron spectrometer. Electrochemical properties were studied by three electrode system using Biologic instruments.

## Results and Discussion

The phase and structure of the synthesized composite materials were studied by powder X-ray diffractometer (XRD) analysis as shown in fig 1. The XRD patterns of graphite oxide (fig 1a) shows a sharp peak at  $2\theta = 11.7^\circ$ , corresponds to the (002) plane of the as prepared GO. All peaks of the composite (Fig 1b - 1d) could be indexed to cubic zinc blende structure and very well agree with the standard JCPDS value (893840). No other impurity phases were observed in this material. This confirms that the Co ions did not affect the zinc blende structure. The average particle size of the composite material was calculated by Debye-Scherrer formula, and in the range of 5nm. When the Co ions concentration increases, there is no change in the particle size. Because Vegards law state that the lattice constant is approximately equal to the composition-weighted average of the lattice constants of the pure materials, i.e. the lattice constant is dependent on the alloy composition. It is very clear from the XRD patterns (Fig 1b – 1d), that the broadening of peaks reveals the nanocrystalline behavior of the composite. In the low angle region, the disappearance of GO peak could be found in the composite. Which indicates the complete exfoliation of graphite oxide in the composite material and (002) plane of reduced graphene oxide might be shield by the (111) plane of CdS nanoparticles.

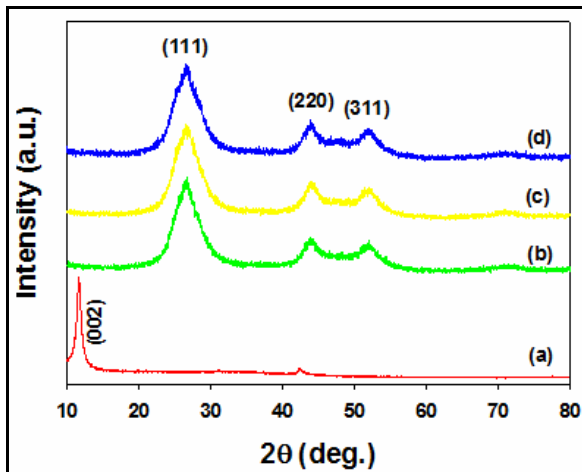


Fig 1. XRD patterns of (a) GO, (b) CdS/rGO, (c) Cd<sub>0.95</sub>Co<sub>0.05</sub>S/rGO, (d) Cd<sub>0.90</sub>Co<sub>0.10</sub>S/rGO composites

The functional groups and the formation of rGO in the composites were studied by FTIR spectral analysis as shown in the fig 2. The oxygen containing functional groups, such as carbonyl, epoxy, hydroxyl and carboxyl groups were present at 1063 cm<sup>-1</sup>, 1223 cm<sup>-1</sup>, 1366 cm<sup>-1</sup> and 1729 cm<sup>-1</sup>. The skeletal vibration of unoxidized domains peak appeared at 1617 cm<sup>-1</sup>. Compared to the GO spectra, the spectrum of composites (fig 2b – 2d) shows the disappearance of the oxygen containing functional groups such as, carboxyl peak at 1729 cm<sup>-1</sup> and the hydroxide group at 1366 cm<sup>-1</sup>. It can be clearly seen that the skeletal vibration peak of graphene was at 1551 cm<sup>-1</sup> and shows the partial presence of remaining alkoxy and epoxy groups were at 1063 cm<sup>-1</sup> and 1233 cm<sup>-1</sup> respectively<sup>10</sup>. The peaks at 604 cm<sup>-1</sup> and 812 cm<sup>-1</sup>, correspond to the CdS nanoparticles<sup>11</sup>. This result suggests that GO was transformed to rGO and the presence of CdS nanoparticles in the composites.

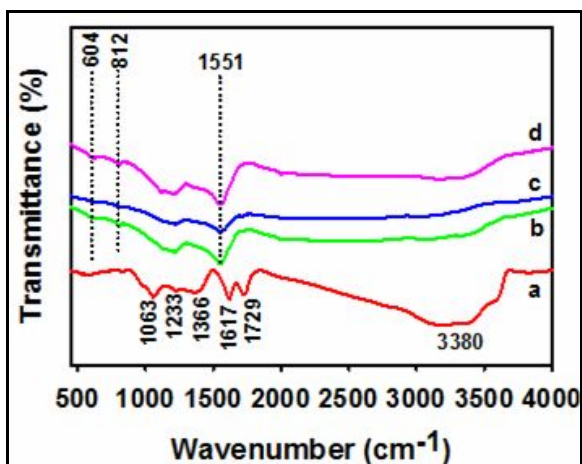


Fig. 2 FTIR spectra of (a) GO, (b) CdS/rGO, (c) Cd<sub>0.95</sub>Co<sub>0.05</sub>S/rGO, (d) Cd<sub>0.90</sub>Co<sub>0.10</sub>S/rGO composites

Raman Scattering is very sensitive to the microstructure of nanocrystalline materials. Fig 3 shows the Raman spectrum of GO and all the composites. With regard to the Raman spectra of GO (Fig 3a), the D band and G band were present at 1354 and 1595 cm<sup>-1</sup>, respectively. All the composite materials (Fig 3b – 3d), the bands at 298.59 and 593.25 cm<sup>-1</sup> corresponding to first longitudinal optical (1LO) and second longitudinal optical (2LO) phonon modes of CdS nanoparticles, respectively and D & G bands of rGO sheets. Compared with the Raman spectra of GO, there is no shift in D-band and G-band shift towards lower wavenumber about 10cm<sup>-1</sup> (1595 cm<sup>-1</sup> to 1585 cm<sup>-1</sup>). The intensity D/G ratio value of all the composites is larger than that of GO suggesting that the reduction of GO hybrids cause reconstruction of some graphene networks<sup>12</sup>.

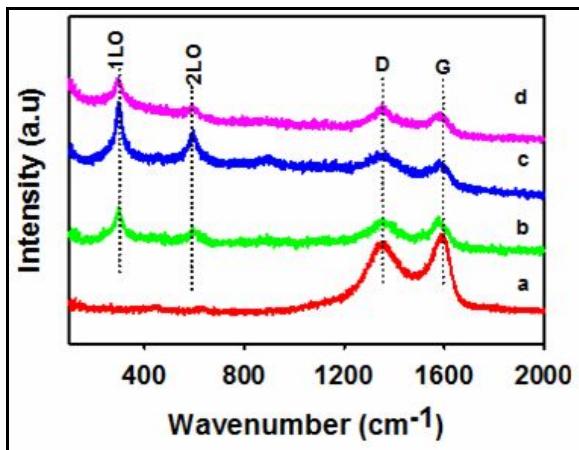


Fig. 3 Raman spectra of (a) GO, (b) CdS/rGO, (c) Cd<sub>0.95</sub>Co<sub>0.05</sub>S/rGO, (d) Cd<sub>0.90</sub>Co<sub>0.10</sub>S/rGO composites

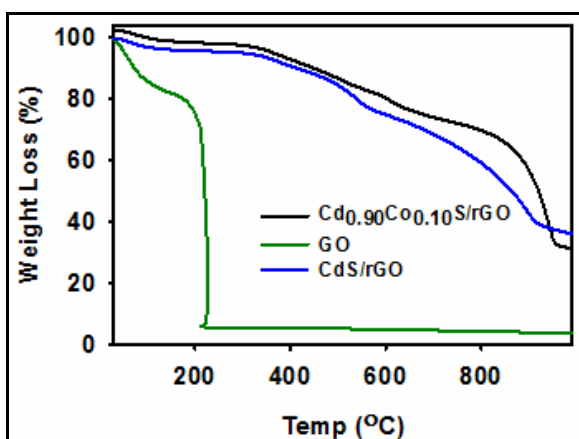
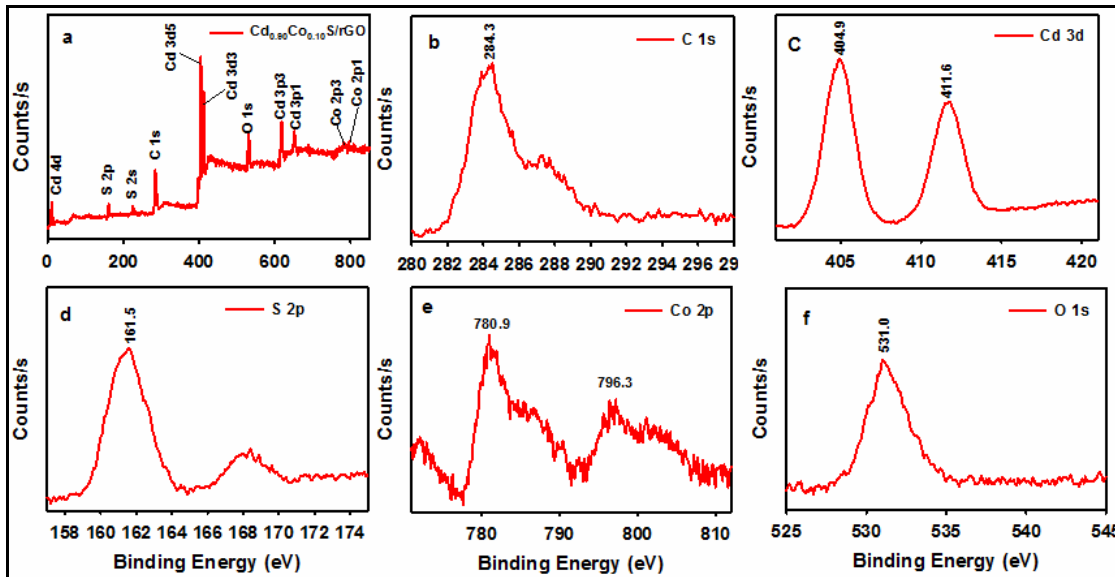


Fig. 4 TGA curves of GO, CdS/rGO, Cd<sub>0.90</sub>Co<sub>0.10</sub>S/rGO composites

The thermal stability of GO, CdS/rGO and Cd<sub>0.90</sub>Co<sub>0.10</sub>S/rGO composite were investigated with TG analysis as shown in fig 4. For GO, below 100 °C weight loss is due to the removal of absorbed water molecules and around 220 °C, the major weight loss is attributed to the decomposition of oxygen containing functional groups. For both the composites, the weight loss below 100°C, which can be attributed to the loss of absorbed water molecules. The small amount of weight loss from 100°C to 300°C can be attributed partial presence of oxygen containing functional groups, and shows the much higher thermal stability with a gradual weight loss up to 800°C compared than GO and CdS/rGO composites. After 800°C, an abrupt weight loss occurs due to the decomposition of CdS nanoparticles. This is consistent with the thermal behavior of pure graphene in N<sub>2</sub> nitrogen atmosphere as reported <sup>11</sup>.

To investigate the elemental composition and their binding energies of GO, rGO/CdS and Cd<sub>0.90</sub>Co<sub>0.10</sub>S/rGO composite, we carried out by X-ray photoelectron spectroscopy (XPS) measurements. Fig. 5a shows the full survey spectrum of Cd<sub>0.90</sub>Co<sub>0.10</sub>S/rGO composite, which confirms the presence of C, O, Cd, Co and S elements. In Fig. 5b, the high intense peak attributed to sp<sup>2</sup> of C = C bond around 284.3 eV. Fig. 5c, shows the Cd doublet peak (Cd 3d<sub>5/2</sub> and Cd3d<sub>3/2</sub>) were present at 404.9 and 411.6 eV with the energy separation value of 6.7 eV. The peak at 161.5 eV corresponds to the S 2p core level as shown in Fig. 5d. The Fig. 5e shows Co 2p peak at 780.9 and 796.3 eV, with the energy separation value of 15.4 eV. In the fig. 5f, the peak at 530 eV corresponds to O 1s.



**Fig. 5** XPS spectrum of  $\text{Cd}_{0.90}\text{Co}_{0.10}\text{S/rGO}$  composites (a) survey, (b) C 1s, (c) Cd 3d, (d) S 2p, (e) Co 2p and (f) O 1s

Fig. 6 Show the Field emission scanning electron microscope and TEM images of all composites. From the TEM images of the composites, it was observed that the  $\text{Cd}_{(1-x)}\text{Co}_{(x)}\text{S}$  spherical nanoparticles deposited on the reduced graphene oxide sheets in a relatively high density. It can be seen that the rGO is not perfectly flat and some very small particles were observed on the surface of rGO sheets.

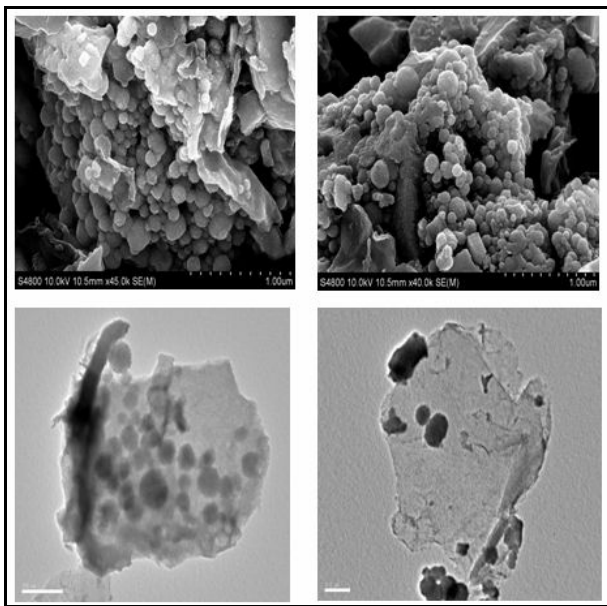


**Fig. 6** SEM & TEM images of (a)  $\text{Cd}_{0.95}\text{Co}_{0.05}\text{S/rGO}$ , (b)  $\text{Cd}_{0.90}\text{Co}_{0.10}\text{S/rGO}$  composites

Fig. 7 shows the CV measurements and were carried out with a three electrode system using glassy carbon electrode, Ag/AgCl electrode and platinum wire as the working electrode, reference electrode and counter electrode respectively and 0.1 M  $\text{KNO}_3$ , 5 mM  $\text{Fe}(\text{CN})_6^{4-}$  and 5 mM  $\text{Fe}(\text{CN})_6^{3-}$  is used as an electrolyte solution. Figure 8 show the CVs of  $\text{Cd}_{0.90}\text{Co}_{0.10}\text{S/rGO}$  composites were performed at a scan rate of 10, 50 and 100 mV/s. The weights of the electrocatalysts were controlled to be the same on each electrode. The CV cycle at every scan rate shows a couple of redox (oxidation and reduction) peaks due to the redox reaction of  $\text{Fe}^{3+}/\text{Fe}^{2+}$ . A pair of redox peaks emerged with an anodic peak potential at about 0.55V and a cathodic peak potential at 0.48V. When the scan rate increases, the anodic peak potential increases, meanwhile the cathodic part turn to be lower.

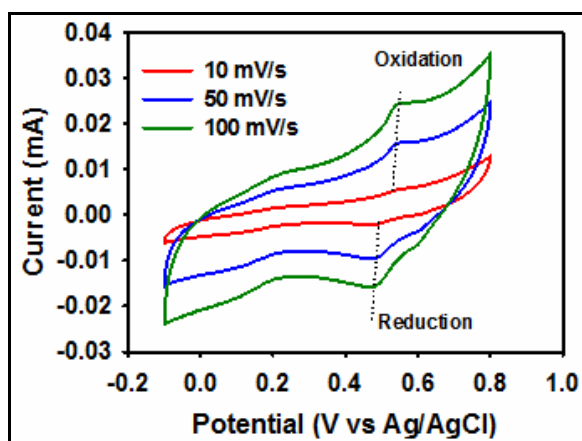


Fig. 7 CV curves of the  $\text{Cd}_{(0.90)}\text{Co}_{(0.10)}\text{S/rGO}$  modified electrode at different scan rates: 10 mV/s, 50 mV/s and 100 mV/s

## Conclusion

$\text{Cd}_{(1-x)}\text{Co}_{(x)}\text{S/rGO}$  composites were synthesized through easy and simple co-precipitation method. The XRD analysis reveals that undoped and doped composites show the same particle size and exhibit the cubic zinc blende structure.  $\text{Cd}_{0.90}\text{Co}_{0.10}\text{S/rGO}$  showed good thermal stability compared with that of GO and  $\text{CdS/rGO}$  composites. FTIR and Raman spectroscopy analysis confirm the formation as well as the reduction of the composites. The binding energy and the presence of elements in the composites were analyzed by X-ray photoelectron spectroscopy. The  $\text{Cd}_{(1-x)}\text{Co}_{(x)}\text{S}$  nanoparticles were deposited on the surface of reduced graphene oxide sheets were characterized by FE-SEM and TEM analysis. CV analysis indicated an increase in the electrochemical current of composite. This novel material will be useful for optoelectronics and energy based applications.

## References

1. Han. W, Ren. L, Gong. L, Qi. X, Liu. Y, Yang. L, Wei. X, and Zhong. J., Self assembled three-dimensional graphene-based aerogel with embedded multifarious functional nanoparticles and its excellent photoelectrochemical activities, *ACS sus. Chem. and Eng.*, 2014, 2, 741-748.
2. Han. W, Ren. L, Qi. X, Liu. Y, Wei. X, Huang. Z, and Zhong. J., Synthesis of  $\text{CdS/ZnO}$ /graphene composite with high efficiency photoelectrochemical activities under solar radiation, *Appl. Surf. Sci.*, 2014, 299, 12-18
3. Lavanya. T, Satheesh. K, Dutta. M, Jaya. N.V, and Fukata. N., Superior photocatalytic performance of reduced graphene oxide wrapped electrospun anatase mesoporous  $\text{TiO}_2$  nanofibers, *J. Alloys and Comp.*, 2014, 615, 643-650
4. Satheesh. K. and Jayavel. R., Synthesis and electrochemical properties of reduced graphene oxide via chemical reduction using thiourea as a reducing agent, *Mat. Lett.*, 2013, 113, 5-8
5. Xu C.H, Wang X.B, Wang J.C, and Hu H.T., Synthesis and photoelectrical properties of b-cyclodextrin functionalized graphene materials with high bio-recognition capability, *Chem. Phy. Lett.*, 2010, 498, 162-167
6. Xiaobo C, and Samuel S.M., Titanium dioxide nanomaterials: synthesis, properties, modifications, and applications. *Chem Rev.*, 2007, 107, 2891-959.
7. Meng N, Michael K.H. L, Dennis Y.C.L, and Sumathy K., A review and recent developments in Photocatalytic water-splitting using  $\text{TiO}_2$  for hydrogen production. *Renewable Sustain Energy Rev.*, 2007, 11, 401-425.
8. Pearton S.J, Norton D.P, Ip K, Heo Y.W, and Steiner T. Recent progress in processing and properties of  $\text{ZnO}$ . *Superlattices Microstruct.*, 2003, 34, 3-32.

9. Satheesh K, Lavanya T, Mrinal D, Jayavel R. and Naoki F., Thiourea assisted one-pot easy synthesis of CdS/rGO composite by the wet chemical method: Structural, optical, and photocatalytic properties, *Ceramics Int.*, 2013, 39, 9207 - 9214
10. Xu Y.X, Bai H, Lu G.W, Li C, and Shi G.Q., Flexible graphene films via the filtration of water-soluble non covalent functionalized graphene sheets, *J. of Amer. Chem. Soc.*, 2008, 130, 5856–5857.
11. Stankovich. S, Dikin D.A, and Piner R.D., Synthesis of graphene - based nanosheets via chemical reduction of exfoliated graphite oxide, *Carbon* , 2007, 45, 1558–1565.
12. Song. S, Gao W, Wang X, Li X, Liu D, Xing. Y, and Zhang. H, Microwave-assisted synthesis of BiOBr/graphene nano composites and their enhanced Photocatalytic activity, *DaltonTransactions.*, 2012, 41, 10472–11076.

\*\*\*\*\*